Development of an analytical methodology using Fourier transform mass spectrometry to discover new structural analogs of wine natural sweeteners

Axel Marchal [a,b,*], Eric Génin [c], Pierre Waffo-Téguo [d], Alice Bibès [a,b], Grégory Da Costa [d], Jean-Michel Mérillon [d], Denis Dubourdieu [a,b]

[a] Univ. de Bordeaux, ISVV, EA 4577, Unité de recherche OENOLOGIE, F-33882 Villenave d'Ornon, France

[b] INRA, ISVV, USC 1366 OENOLOGIE, 33882 Villenave d'Ornon, France

[c] Thermo Fisher Scientific, LC/MS Laboratory, 16 avenue du Québec, F-91140 Villebon sur Yvette, France

[d] Univ. de Bordeaux, ISVV, GESVAB, EA 3675, F-33882 Villenave d'Ornon, France

Corresponding author:

Axel Marchal

axel.marchal@u-bordeaux.fr

Abstract:

Volatile and non-volatile molecules are directly responsible for the thrill and excitement provided by wine-tasting. Their elucidation requires powerful analytical techniques and innovative methodologies. In a recent work, two novel sweet compounds called quercotriterpenosides (QTT) were identified in oak wood used for wine-ageing. The aim of the present study is to discover structural analogs of such natural sweeteners in oak wood. For this purpose, an analytical approach was developed as an alternative to chemical synthesis. Orbitrap mass spectrometry proved to be a crucial technique both to demonstrate the presence of QTT analogs in oak wood by targeted screening and to guide the purification pathway of these molecules using complementary chromatographic tools. Four compounds were isolated and identified for the first time: two isomers, one glucosyl derivative and one galloyl derivative of QTT. Their tasting showed that only the two new isomers were sweet, thus demonstrating both the pertinence of the strategy and the influence of functional groups on gustatory properties. Finally, this paper presents some developments involving multistage Fourier transform mass spectrometry (FTMS) to provide solid structural information on these functional groups prior to any purification of compounds. Such analytical developments could be particularly useful for research on taste-active or bio-active products.

Keywords: Sweetness, High resolution mass spectrometry, Triterpenes, Oak wood, Liquid chromatography

Highlights

An analytical approach based on HRMS targeted screening was developed to search for structural analogs of sweeteners.

The purification protocol using CPC and HPLC was guided by HRMS.

Four new triterpenoids were identified in oak wood, two of them were sweet.

Structural information on nature, position and sequence of functional groups were provided by $HRMS^n$ developments.

1. Introduction

Beyond its economic and cultural importance, wine is an object of fascination for tasters around the world, sparking their interest and emotion through the variety of its organoleptic qualities [1]. This wide sensory diversity is due to a great chemical complexity, since wine contains thousands of molecules evolving constantly and stimulating the senses of the taster [2]. Some of them, called key compounds, have a decisive contribution to the odor and flavor of the wine. Oenological research has helped to discover some but many remain unknown [3]. Indeed, knowledge about the chemical composition of wine and about natural products in general can be gained only if the analytical methods available to researchers are improved. Thus, the analytical chemist is akin to a translator since his role is to decrypt the chemical basis of the sensory language transmitted by the wine to the taster [4]. With the development of gas chromatography techniques used by flavorists [5], [6], many volatiles were found in wines [3], [7], [8]. Contrary to odors, the molecular determinants of tastes (other than organic acids) remain much less known. Nevertheless, the development of analytical methods applied to the study of natural products has resulted in significant work on non-volatiles in wine over the last decades [9], [10], [11], [12], [13].

Recently, many studies have utilized the great potential of high resolution mass spectrometry (HRMS) in the study of wine [14], [15], [16], [17]. Most of them have adopted a 'metabolomic-type' approach. This is particularly powerful because it provides a general fingerprint of wine, but it does not necessarily allow compounds with interesting organoleptic properties to be specifically targeted. We have already used Fourier transform mass spectrometry (FTMS), a high resolution technique, to identify sweet compounds from oak wood [18]. Their chemical nature was previously unknown and they were isolated by using a 'taste-guided' inductive method. These studies have led to significant advances in wine flavor knowledge by discovering two new triterpenoids named quercotriterpenosides I and II.

Decreasing carbohydrate intake is a major public health issue so when a high-potency sweetener is identified, it is common to search for structural analogs with similar, or even more interesting, properties [19], [20], [21]. In general, chemical synthesis is involved in generating these analogs by making slight modifications to the stereochemistry or substituents of the sweetener [22], [23], [24], [25]. However, natural biosynthetic pathways may also cause changes of the same type and several isomers and derivatives of a natural compound are often observed in the same plant [26].

How can we take benefit from the wide diversity of molecules naturally biosynthesized in the plant kingdom? This study proposes an innovative alternative to chemical synthesis in the search for structural analogs of **QTT I** and **II**. The originality of this approach relies on the implementation of targeted analysis to explore the chemical diversity due to the biosynthetic pathways in oak wood. Instead of synthesizing isomers or derivatives of QTT, we aimed at isolating such compounds from a natural source. For this purpose, FTMS using an Orbitrap analyzer was coupled with U-HPLC (ultra high-performance liquid chromatography) to perform targeted screening and to search for isomers and derivatives of these molecules on the basis of their empirical formula. This powerful analytical technique was also used to guide purification of the target compounds (TC), whose structure was further determined by nuclear magnetic resonance (NMR). The implementation of this strategy led to the isolation and identification of four new triterpenoids. Finally, fragmentation by multistage high-resolution mass spectrometry ($HRMS^n$) showed the value of this tool to provide critical structural information likely to simplify the interpretation of bidimensional NMR (2D NMR). Such molecular elucidation generally requires previous and fastidious isolation of compounds, but we demonstrate here that reliable information can be obtained directly from the complex matrix by coupling liquid chromatography (LC) with $HRMS^n$ prior to any purification. Beyond furthering knowledge of wine flavor compounds, these results open up promising perspectives for the study of natural compounds using LC-FTMS.

2. Materials and methods

2.1. Chemicals and materials

Oak heartwood used in this study came from staves of *Quercus petraea* grown in various French forests (Centre, Vosges, Allier) and seasoned outside, without shelter, during two years. The staves were reduced to chips (30 mm × 20 mm × 5 mm) by the cooperaging industry (Seguin Moreau, Merpins, France). All solvents were HPLC grade (VWR International, Fontenay-sous-Bois, France) except acetonitrile used for HRMS analysis (Optima® LCMS grade, Fisher Scientific, Fair Lawn, USA) and deionized water (MilliQ, Millipore, Bedford, USA). **QTT I** and **II** were isolated from an oak wood extract by combining centrifugal partition chromatography fractionation and high performance liquid chromatography purification according to the procedure described by Marchal et al. [18].

112 *2.2. Extraction and preparation of the pre-purified extract*

113

114 A batch of wood chips (1 kg) was extracted with ethanol/water (60/40 v/v; 4 L) for 7
115 days at room temperature. After filtration (0.45 µm), the liquid medium was concentrated *in*
116 *vacuo* to remove ethanol. The aqueous solution (800 mL) was washed with *n*-heptane (3 × 300
117 mL) and then extracted with ethyl acetate (5 × 400 mL). The combined organic layers were
118 evaporated under reduced pressure, suspended in water and freeze-dried twice to obtain 6 g of
119 pre-purified extract.

120

121 *2.3. FT/MS*

122

123 Two Fourier transform mass spectrometers were used in this study with the following
124 configurations for direct injection (DI) and LC-FTMS applications.

125

126 *2.3.1. Exactive® configuration*

127 The Exactive platform consisted of an HTC PAL® autosampler (CTC Analytics AG,
128 Zwingen, Switzerland), an Accela U-HPLC system with quaternary pumps and an Exactive
129 Orbitrap mass spectrometer equipped with a heated electrospray ionization (HESI I) probe (both
130 from Thermo Fisher Scientific, Bremen, Germany).

131

132 *2.3.2. LTQ-Orbitrap Elite® configuration*

133 The LTQ-Orbitrap Elite platform consisted of a Thermo Scientific Dionex Ultimate
134 3000 RSLC autosampler, a quaternary pump and the LTQ-Orbitrap Elite mass spectrometer
135 equipped with a heated electrospray ionization (HESI II) probe (both from Thermo Fisher
136 Scientific, Bremen, Germany). Collision induced dissociation (CID) MS^2 and MS^3 studies were
137 performed in the Linear Ion Trap (LIT). In addition, non-resonant activation was also carried
138 out in the Higher Collisional Energy (HCD) cell situated at the far end of the C-Trap region
139 [27]. In both cases, the product ions were detected in the Orbitrap analyzer in order to generate
140 high mass accuracy data. Indeed, all the ions were detected with mass errors in the 1 ppm range
141 [28].

142

143 *2.3.3. LC-FT/MS conditions*

144 Both spectrometers were calibrated using Pierce® ESI Negative and Positive Ion
145 Calibration solutions (Thermo Fisher Scientific) before each series of analyses.

Direct infusion analysis was performed on the LTQ-Orbitrap spectrometer. The sample was dissolved to 10 mg L^{-1} in CH_3OH/H_2O 1:1 (v/v) and delivered by a syringe pump with a flow rate of 5 µL min^{-1}.

Both the Exactive and LTQ-Orbitrap systems were used for LC-FT/MS analysis. For liquid chromatography separation, a C18 column was used as the stationary phase (Hypersil Gold 2.1 mm × 100 mm, 1.9 µm particle size, Thermo Fisher Scientific). The mobile phases were (A) water + 0.1% formic acid and (B) acetonitrile + 0.1% formic acid. The flow rate was 600 µL min^{-1} and eluent B varied as follows: 0 min, 18%; 0.5 min, 18%; 4 min, 45%; 4.2 min, 98%; 6.4 min, 98%; 6.5 min, 18%; 7.5 min, 18%. Injection volume was 5 µL. Ionization and spectrometric conditions are summarized in Table 1.

All data were processed using the Qualbrowser application of Xcalibur version 2.1 (Thermo Fisher Scientific).

2.4. Fractionation of pre-purified extract and isolation of targeted compounds

2.4.1. Centrifugal partition chromatography (CPC) apparatus

Purification was performed on a Spot prep II LC system equipped with SCPC-100+1000 (Armen Instrument, Saint-Avé, France). Fractionation was performed on a 1000 mL rotor made of 21 stacked disks with a total of 1512 twin cells, 524.5 µL per cell, a total active volume of 1000 mL, and a dead volume of 207 mL. The rotation speed could be adjusted from 0 to 2000 rpm. The solvent was pumped into the column by a 4-way quaternary high-pressure gradient pump (flow rates and pressures of up to 250 mL min^{-1} and 230 bars possible respectively). The samples were introduced into the CPC column via an automatic high pressure injection valve. Continuous monitoring of the effluent was performed with an ECOM Flash 06 diode array detector equipped with a preparative flow cell. Fractions were collected by the fraction collector of the spot prep II. The system was controlled by Armen Glider Prep V5.0 software. All the experiments were conducted at room temperature.

2.4.2. CPC separation procedure

The biphasic solvent system used for the fractionation of the pre-purified extract was the Arizona-G system [29]. The biphasic system was prepared by thoroughly mixing *n*-heptane (800 mL), ethyl acetate (EtOAc, 3200 mL), methanol (MeOH, 800 mL) and water (H_2O, 3200 mL) in a separating funnel at room temperature, shaking vigorously and allowing it to settle until the phases became limpid. The resulting two phases were separated just before use.

The CPC column was first filled with 2.5 L of the lower aqueous stationary phase at 30 mL min^{-1} and at 300 rpm. The upper mobile phase in ascending mode was pumped into the column at a flow-rate of 20 mL min^{-1} with a rotor rotation of 1400 rpm. After the mobile phase emerged and the thermodynamic equilibrium was reached (percentage of retention of the stationary phase 74%), the sample solution containing 6 g of dry pre-purified extract dissolved in 25 mL of a mixture consisting of upper and lower phase (1:2, v/v) were injected through a 30 mL loop.

The content of the outgoing mobile phase was monitored by UV detection at 254 and 280 nm. The system was switched to descending mode after 170 min. The heavier aqueous phase was pumped at 40 mL min^{-1}. The fraction collector was set at 1 tube min^{-1} during ascending mode (from 0 to 170 min) and at 2 tubes min^{-1} during descending mode (from 170 to 200 min). The whole experiment lasted 200 min and was performed at room temperature (±20 °C).

Every five CPC tubes, 10 µL were taken, evaporated and dissolved in 1 mL of H_2O/MeOH 95/5. After filtration (0.45 µm), 5 µL of each sample were injected in LC-HRMS using the Exactive spectrometer. According to LC-HRMS results, CPC tubes were pooled, evaporated in vacuo, suspended in water and freeze-dried.

2.4.3. HPLC purification

Final purification of the compounds was performed on a C18 preparative column (Microsorb 100-5 250 mm × 21.4 mm, 5 µm particle size, Varian) with a pre-column (Prontosil C18 5 µm 50 mm × 20 mm, Bischoff chromatography). Solvents (A water and B acetonitrile, both containing 0.05% trifluororacetic acid) were pumped by a Prostar 218 2-way binary high-pressure gradient pump (Varian). The flow rate was 20 mL min^{-1}.

To purify **TC 1**, **3** and **4**, eluent B followed this gradient: 0 min, 25%; 7 min, 25%; 40 min, 30%; 42 min, 100%; 50 min, 100%. To purify **TC 2**, eluent B followed this gradient: 0 min, 18%; 6 min, 18%; 18 min, 26%; 23 min, 26%; 31 min, 32%; 36 min, 32%; 53 min, 48%; 55 min, 100%; 62 min, 100%. Aliquots (20 mg) of CPC fractions were dissolved in methanol (200 µL), filtered and manually introduced into the system.

UV detection was carried out at 254 and 280 nm by a Prostar 345 detector (Varian). Chromatographic peaks were manually collected just downstream the detector. Samples obtained after successive injections were pooled, evaporated *in vacuo* to remove acetonitrile and freeze-dried twice to obtain white amorphous powders.

214 *2.5. Sensory assessment*

215

216 After purification, **TC 1**, **2** and **4** as well as **QTT I** and **II** were individually dissolved
217 at 5 mg L^{-1} in a 12% vol. alc. hydro-ethanolic solution as well as in a white non-oaked wine
218 (Bordeaux, 2011). The hydro-ethanolic solution was composed of pure and demineralized water
219 (eau de source de Montagne, Laqueuille, France) and distilled ethanol. The samples were tasted
220 by six experts in wine tasting. They described the gustatory perception of each compound using
221 the vocabulary of wine tasting. In particular, the sweetness intensity was evaluated on a scale
222 from 0 (not detectable) to 5 (strongly detectable) and compared to **QTT I** and **II** perception.

223

224 *2.6. NMR experiments*

225

226 All 1D and 2D NMR experiments were performed on a Bruker Avance 600 MHz NMR
227 spectrometer operating at 600.3 MHz and equipped with a 5 mm TXI probe. Data were
228 processed using TOPSPIN software (Bruker Topspin). All NMR spectra were acquired in
229 methanol-*d*4. ^{1}H and ^{13}C chemical shifts were referenced to solvent signals, δ (^{1}H) 3.31 and δ
230 (^{13}C) 49.1. Spectra were collected at 300 K and data were processed using TOPSPIN software
231 (Bruker).

232 Molecule assignments were achieved by two-dimensional ^{1}H-^{1}H COSY, ^{1}H-^{1}H
233 ROESY, ^{1}H-^{13}C HSQC, ^{1}H-^{13}C HSQC-TOCSY [30], and ^{1}H-^{13}C HMBC experiments. All 2D-
234 experiments were carried out with 2048 data points ×256 increments and a spectral width of
235 7211 Hz and 31,700 Hz in proton and carbon dimension respectively, 128 scans and 1.5 s for
236 relaxation delay. Mixing time was 400 ms and the spinlock time was 150 ms for ROESY and
237 HSQC-TOCSY experiments, respectively.

238

239 ## 3. Results and discussion

240

241 *3.1. Targeted screening of oak wood extract and purification of QTT isomers and derivatives*
242 *guided by LC-HRMS*

243

244 The mass accuracy specifications of the Orbitrap analyzer make it possible to target *m/z*
245 ions corresponding to given empirical formulae. In this study, we used an Exactive spectrometer
246 to search for isomers and derivatives of **QTT I/II**. We screened an oak wood macerate by

constructing extracted ion chromatograms (XIC) in a 5 ppm window around the empirical formulae shown in Table 2.

XIC for **QTT I/II** isomers showed three dominant peaks: a major peak at retention time (RT) 3.72 min and two peaks at 3.31 and 4.02 min, the latter two corresponding respectively to **QTT I** and **II** as demonstrated by comparison of RT with pure compounds (Fig. 1). XICs of MonoHex and MonoGall derivatives showed in each case one dominant peak at 3.60 and 3.78 min, respectively. No significant chromatographic peaks were observed for DiHex DiGall and MonoHex-MonoGall derivatives.

In summary, targeted screening revealed the presence of isomers and derivatives of sweet **QTT I/II** in the oak wood extract. Our goal was to purify the dominant species of each XIC to confirm their triterpenoid nature, identify their chemical structure and assess their sensorial properties. At this step, these compounds were called **TC**s (target compounds) **1**, **2** and **3** for isomers, MonoHex and MonoGall derivatives, respectively (Fig. 1). Owing to the chemical complexity of the oak wood matrix, complementary separation techniques were implemented to obtain purification of TCs.

3.2. LC-HRMS-guided purification of target compounds

Various fractionation steps were necessary to isolate the TCs and LC-HRMS was used at each step to guide the purification pathway. First, the crude hydro-ethanolic extract was pre-cleaned by solvent extraction in order to enrich it in TCs. LC-HRMS analysis indicated that the TCs were mainly present in the ethyl acetate organic layer. Then, this pre-purified extract was submitted to preparative CPC separation with the ARIZONA-G system composed of *n*-heptane/EtOAc/MeOH/H_2O (1:4:1:4, v/v) to obtain 230 tubes in 200 min (Fig. S1 Supplementary data).

After the CPC experiment, LC-HRMS analysis of CPC tubes allowed the constitution of fractions enriched in target compounds. To facilitate further purification, tubes were pooled on the basis of their chemical composition by making a compromise between abundance and purity of target triterpenoids: tubes 78–104 for **TC1** and **TC3** (158 mg), tubes 203–209 for **TC2** (47 mg).

Although the TCs were not pure in the CPC fractions, the CPC experiment allowed efficient fractionation of the pre-purified oak extract so purification was easily achieved by preparative HPLC using water/acetonitrile gradients adapted for each fraction (Figs. S2 and S3 in Supplementary data). The target compounds were well separated and obtained as white

powder (**TC1**, 17 mg; **TC2**, 4.8 mg; **TC3**, 1.1 mg). Moreover, HPLC purification of CPC fractions 78–104 exhibited a small peak at 26.7 min (Fig. S2 in Supplementary data). LC-HRMS analysis showed that this compound was another isomer of **QTT I** and **II**. It was previously co-eluted with **TC1** in U-HPLC. After HPLC separation, this compound was obtained as a pure white powder (4.3 mg) and called **TC4**.

Consequently, implementation of CPC and HPLC fractionation guided by targeted LC-HRMS analysis were complementary. They made it possible to purify four compounds with an empirical formula corresponding to isomers and derivatives of sweet **QTT I** from a highly complex matrix. The LC-HRMS analysis of each pure compound showed retention times similar to those observed in Fig. 1 (data not shown). Consequently, the dominant species of each XIC have in fact been purified, which validates the isolation method.

Furthermore, it is interesting to note that the retention times of **TC1** and **TC2** were almost co-eluted in LC-HRMS (respectively 3.72 and 3.60 min), whereas they were about 110 min different in CPC. **QTT I**, **QTT II**, **TC1**, **TC3** and **TC4** were eluted in ascending mode and **TC2** in descending mode. Indeed, the modalities of separation appropriate to CPC and HPLC are different [31], [32]. HPLC has a high number of theoretical plates (N) and a low volume of stationary phases, whereas CPC has a low number of plates but a high volume of stationary phases so it can act on the selectivity factor [33]. Whereas CPC involves only liquid phases, HPLC separation functions with a solid support as stationary phase. Consequently, HPLC selectivity depends primarily on a partition mechanism between the mobile phase and the chemically bonded stationary phase, which in this case was C18, but it is also influenced by secondary mode interactions with the support matrix (silica). Indeed, the combination of CPC and preparative HPLC was efficient to purify the target compounds from a complex mixture of oak with different polarities and contents because of their complementary and orthogonal properties.

3.3. Structural elucidation of new isomers and derivatives of sweet QTT I and II

Compounds were purified according to HRMS analysis by searching for ions with characteristic *m/z* ratios in a 5 ppm window. Consequently, the empirical formula of these compounds was known but not their structural formula. Their identification was assumed by mono- and multidimensional NMR spectroscopy (Table 3, Fig. S4 Supplementary data).

TC1 was obtained as a white amorphous powder with a quasi-molecular $[M–H]^-$ ion peak at *m/z* $[M–H]^-$ 817.4012 in negative mode in the HRMS spectrum, in agreement with the

molecular formula of $C_{43}H_{61}O_{15}$ (0.5 ppm). ^{1}H and ^{13}C NMR data of **TC1** (Table 3) were very close to those of **QTT I** and **II**, which were recently published [18]. The ^{1}H NMR spectra of **TC1** exhibited signals of an olefinic proton at δ 5.36 (*t*, *J* = 3.3 Hz, H-12), six methyl singlets at δ 0.79 (H-26), 0.86 (H-24), 0.96 (H-30), 0.97 (H-29), 1.11 (H-25), 1.34 (H-27), five oxygen-bearing methine protons at δ 3.99 (*td*, *J* = 4.7 and 11.5 Hz, H-2), 5.05 (*d*, *J* = 9.9 Hz, H-3), 3.29 (*d*, *J* = 4.1 Hz, H-19), and a primary alcohol function at δ 3.01 (*d*, *J* = 11.9 Hz) and 3.32 (*d*, *J* = 11.9 Hz), suggesting the presence of arjungenin as the triterpenoid moiety (Fig. S4 in Supplementary data). The corresponding carbons were identified by an HSQC experiment. Comparison of the NMR data of **TC1** with **QTT I** indicated that the position C-3 (δ 78.7) of arjungenin is substituted. The HMBC spectrum showed cross-peaks between H-3 (δ 5.05) of the arjungenin and C-7″ (δ 167.5) of the galloyl group, confirming the transfer of the galloyl unit from C-23 to C-3. This suggested that **TC1** is a regioisomer of **QTT I** (Fig. 2). Thus we concluded that the structure was a new triterpenoid, 3-*O*-galloyl arjungenin 28-*O*-β-glucopyranosyl, which we called quercotriterpenoside III (**QTT III**).

TC2 was obtained as a white amorphous powder with a quasi-molecular $[M–H]^-$ ion peak at *m*/*z* $[M–H]^-$ 979.4543 in negative mode in the HRMS spectrum, in agreement with the molecular formula of $C_{49}H_{71}O_{20}$ (0.1 ppm). Two anomeric carbons were detected at δ 94.2 and 104.2 in the ^{13}C NMR spectrum attached to doublets at δ 5.38 (*d*, *J* = 8.1 Hz) and δ 4.51 (*d*, *J* = 8.2 Hz), respectively in the HSQC experiment (Table 3). Analysis of 2D experiments (COSY, ROESY,and HSQC) revealed two β-glucopyranosyl esters and a galloyl group. Owing to the overlapping effects of the signals in the sugar field, HSQC-TOCSY [30] was used to assign accurately the chemical shifts of the sugar moiety (see Fig. S5 in Supplementary data). The cross peaks observed in the HMBC experiment between C-28 (δ 176.9) of the arjungenin and H-1′ of the glucose moiety (δ 5.38), between C-3 (δ 94.4) of the genin and H-1″ of the second sugar (δ 4.51) and between C-7‴ (δ 166.4) of the galloyl group and H-6a″ and 6b″ (δ 4.38 and 4.65) showed that **TC2** is 3-*O*-[(6-*O*-galloyl)-β-glucopyranosyl] arjungenin 28-*O*-β-glucopyranosyl (Fig. 2). Thus we concluded that the structure of **TC2** was a new triterpenoid, which we called Quercotriterpenoside IV (**QTT IV**).

TC3 was obtained as a white amorphous powder with a quasi-molecular $[M–H]^-$ ion peak at *m*/*z* 969.4122 in negative mode in the HRMS spectrum, in agreement with the molecular formula of $C_{50}H_{65}O_{19}$ (0.3 ppm). The ^{1}H and ^{13}C NMR data of **TC3** were closely comparable to those of **QTT I** [18] except for the C-3 signals (Table 3). The C-3 possessed a deshielded proton at δ_H 5.24, indicating the position of the second galloyl unit. The HMBC spectrum showed cross-peaks between H-3 (δ 5.24) of the arjungenin and C-7″ (δ 166.4) of the galloyl

moiety, confirming the position of the second galloyl in C-3. Thus, the structure of **TC3** is 3,23-*O*-digalloyl arjungenin 28-*O*-β-glucopyranosyl (Fig. 2). This compound has never been described in the literature to date so we called it Quercotriterpenoside V (**QTTV**).

TC4 was obtained as a white amorphous powder with a quasi-molecular $[M–H]^-$ ion peak at *m*/*z* 817.4012 in negative mode in the HRMS spectrum, in agreement with the molecular formula of $C_{43}H_{61}O_{15}$ isomeric with **QTT III**. The presence of a glycosyl residue was confirmed from the observation of the signal of the anomeric position at δ_C 94.4 and δ_H 5.39 (J = 8.4 Hz). NMR data indicated that **TC4** had the same glycosidic part as **QTT I** and **III**: a β-glucopyranosyl ester. These results suggested that **TC4** is a regioisomer of **QTT I** and **III** with the galloyl unit attached to C-2 of the arjungenin instead of C-3 (Table 3). Thus we concluded that **TC4** was 2-*O*-galloyl arjungenin 28-*O*-β-glucopyranosyl (Fig. 2). This compound has never been described in the literature to date so we named it Quercotriterpenoside VI (**QTT VI**).

The molecular elucidation of **TC 1**–**4** confirmed that these molecules were QTT derivatives; thereby validating the approach developed in this study to search for structural analogs of sweet **QTT I**. The discovery of four new triterpenoids supplements knowledge about oak wood composition, but above all illustrates the chemical diversity offered by biosynthetic pathways. To assess their sensory properties, the newly identified **QTT III**, **IV** and **VI** were then individually tasted by six experts at 5 mg L^{-1} in a hydro-ethanolic solution (12% alc. v/v) and in a white wine. They described the gustatory perception of each compound solution in comparison with a control medium solution and with **QTT I** and **II**. The amount of **QTT V** was too low to be tasted. As previously described, **QTT I** was sweet and was rated 5/5. Sensory analysis revealed that its three other isomers, i.e., **QTT II**, **III** and **VI** also exhibited sweetness with a rated intensity of 3, 3 and 5, respectively. Conversely, **QTT IV** did not clearly exhibit any sweet taste but showed a slight mouthfulness. Therefore, among the compounds isolated from oak wood by using a targeted LC-HRMS approach, two new sweeteners were discovered. These sensory results achieve the original objective of the study and validate consequently the method.

This approach differs from methodologies based on a taste-guided purification which provided highly relevant results in food science [34], [35], [36] and more particularly in wine science [10], [18], [37]. In this work, the compounds were indeed purified on the basis of their elemental composition. Such a targeted screening allows the discovery of molecular taste-markers in wine. This strategy appears therefore complementary to ‘metabolomic-type’ approaches that were successfully applied to wine study to identify general trends involved in

wine quality [16], [38], [39]. Another interesting way to explore might concern the receptor-binding techniques [40] consecutive to the discovery of the human taste receptor to sweetness [41]. These techniques allow high-throughput screening and have been recently used to discover new natural sweeteners [42].

Moreover, it is noteworthy in our results that only the isomers containing one glucosyl and one galloyl moiety exhibited a sweet taste. This suggests the importance of functional groups in the gustatory properties of QTT and its interpretation needs further work on the structure/activity relationship. NMR is a powerful technique for structural identification but its implementation requires previous purification of significant amounts of molecules, which is a limitation for studying natural compounds in complex matrixes. HRMS could therefore become an alternative tool to provide complementary structural information relative to functional groups.

3.4. Multistage high-resolution mass spectrometry ($HRMS^n$) as a reliable source of structural information

HRMS is generally used for accurate mass measurement allowing the determination of unknown natural molecules' elemental composition. Here, we investigated further developments of this powerful technique that could provide information on the molecular structure. Indeed, direct injection (DI) of purified compounds in the LTQ-Orbitrap mass spectrometer allowed generation of fragments by multistage mass spectrometry experiments in LTQ (MS^n) and determination of their molecular composition in the Orbitrap analyzer. Such technology provides reliable structural information about isolated compounds that is complementary to NMR data.

3.4.1. Influence of the galloyl position on MS/MS CID spectra

Collision-induced dissociation (CID) MS^2 spectra of the four isomers **QTT I**, **II**, **III** and **VI** are shown in Fig. 3. All these spectra had an ion $C_{37}H_{51}O_{10}^-$ (theoretical *m/z* 655.3488) corresponding to the loss of a neutral $C_6H_{10}O_5$ moiety, thus confirming the presence of a hexosyl in these compounds [43]. However, the four spectra were different: whereas the MS^2 spectrum of **QTT I** exhibited only this $C_{37}H_{51}O_{10}^-$ ion, the spectra of **QTT II**, **III** and **VI** showed other ions corresponding to $C_{39}H_{53}O_{11}^-$, $C_{37}H_{49}O_9^-$, $C_{36}H_{51}O_8^-$ and $C_{36}H_{49}O_7^-$. The fragment $C_{39}H_{53}O_{11}^-$ (theoretical *m/z* 697.3593) resulted from $C_{43}H_{61}O_{15}^-$ by the loss of a $C_4H_8O_4$ moiety due to the fragmentation of the glucopyranosyl, as frequently observed [44].

The three other fragments corresponded to the loss of the neutral glucosyl moiety together respectively with dehydration (theoretical *m/z* 637.3382), decarboxylation (theoretical *m/z* 611.3589) and dehydration + decarboxylation (theoretical *m/z* 593.3484), presumably occurring on the genin part. Moreover, it is noteworthy that the relative abundances of these ions were not the same in the MS^2 spectra: they were similar for **QTT II** and **III** but both were distinct from **QTT VI**. Consequently, we observed three kinds of distinct MS^2 spectra for the four QTT: **QTT I**, **QTT II/III** and **QTT VI**. These groups correspond to three galloyl positions on the genin, respectively at C-23, C-3 and C-2. These results showed that the position of the galloyl moiety strongly influenced the fragmentation pathway of the quasi-molecular ion in negative mode, so MS^n could be useful to predict this position.

An application of these results is the prediction of the galloyl position in QTT derivatives. Indeed, the CID MS^2 spectrum of the $[M–H]^-$ species of **QTT V** (*m/z* 969.4122 $C_{50}H_{65}O_{19}^-$) showed ions at *m/z* 817.4014 ($C_{43}H_{61}O_{15}^-$), *m/z* 807.3597 ($C_{44}H_{55}O_{14}^-$), and *m/z* 655.3487 ($C_{37}H_{51}O_{10}^-$) attributed respectively to the neutral loss of galloyl, hexosyl and galloyl + hexosyl moieties (Fig. S6 Supplementary data). Therefore the *m/z* 817 species corresponded to the genin functionalized with one hexosyl and one galloyl, as for **QTT I**, **II**, **III** and **VI**. Since the MS^3 spectrum of this *m/z* 817 ion obtained from **QTT V** (Fig. 4) was quite similar to the MS^2 spectra of **QTT II** and **III** (Fig. 3), we concluded that the galloyl group was connected to the C-3 of the genin. Consequently, this MS/MS experiment made it possible to determine the position of one galloyl group in **QTT V**.

The CID MS^2 spectrum of the $[M–H]^-$ species of **QTT IV** (*m/z* 979.4543 $C_{49}H_{71}O_{20}^-$) also showed an ion at *m/z* 817 (Fig. S7 Supplementary data), but its MS^3 spectrum did not resemble any of MS^2 spectra previously obtained for the QTT isomers (Fig. S8 Supplementary data). Therefore, the molecular environment of the galloyl in **QTT IV** seemed to be different from that of other QTTs.

3.4.2. $HRMS^n$ as a tool to determine the nature and sequence of functional groups in QTT IV

Non-resonant HCD fragmentation is useful to determine the functional groups present in a molecule. For example, the HCD 80 eV spectrum of the $[M–H]^-$ ion of **QTT IV** (*m/z* 979.4546 $C_{49}H_{71}O_{20}^-$) showed ions at *m/z* 817.4015 ($C_{43}H_{61}O_{15}^-$), *m/z* 665.3908 ($C_{36}H_{57}O_{11}^-$), *m/z* 503.3381 ($C_{30}H_{47}O_6^-$) and *m/z* 169.0146 ($C_7H_5O_5^-$), thus revealing the presence of 2 hexosyl and 1 galloyl moieties on the arjungenin skeleton (Fig. S9 Supplementary data). Furthermore, the ion at *m/z* 313.0566 ($C_{13}H_{13}O_9^-$) demonstrated that at least one hexosyl was linked to the galloyl group of **QTT IV**.

Resonant CID MS/MS allowed successive fragmentations to provide complementary structural information. A full scan spectrum of **QTT IV** in positive ionization mode exhibited an ion at *m*/*z* 1003.4504 corresponding to $[M + Na]^+$. The MS^3 spectrum of the monodeglucosylated fragment ion at *m*/*z* 841.3982 $[M–Glu + Na]^+$ showed an ion at *m*/*z* 355.0636 ($C_{13}H_{16}O_{10}Na^+$) corresponding to the species $[Glu–Gall + Na]^+$ and showing that the hexose remaining in the ion at *m*/*z* 841 is linked to the galloyl moiety (Fig. 5). Moreover, we observed an ion at *m*/*z* 689.3871 ($C_{36}H_{58}O_{11}Na^+$) corresponding to a degalloylation. Since galloyl and hexosyl groups were linked in the *m*/*z* 841 species and because this species was degalloylated into the *m*/*z* 689 still containing the hexose group, then this MS^3 spectrum demonstrated that the galloyl was not connected to the genin directly but through the hexose. Consequently, such MS/MS fragmentation appears powerful to determine not only the nature but also the sequence of the functional groups.

3.4.3. Comparison of MS/MS spectra obtained by DI-MS and LC-MS

The abovementioned MS spectra were obtained after direct injection of the sample into a mass spectrometer through the ESI probe. This method requires preliminary purification of the compound under study to avoid isobaric interactions or confusion between isomers when selecting the precursor. On the other hand, use of liquid chromatography coupled with mass spectrometry allows the separation of molecules before their MS analysis. CID MS^2 spectra obtained by direct injection of pure **QTT II** and during LC-MS analysis of an oak wood extract at the characteristic retention time of **QTT II** were compared (Supplementary data, Fig. S10 A and B respectively).

The LC-$HRMS^2$ spectrum of **QTT II** was quite similar to that previously obtained by DI. Such results were observed for other compounds and other kinds of spectra (data not shown), thus demonstrating the strong similarity between these two methods: the spectra recorded by LC-$HRMS^n$ were as robust as those obtained by DI-$HRMS^n$. Moreover, liquid chromatography allows separation of molecules consistent with the study of compounds in mixture. Consequently, this study shows that LC-$HRMS^n$ can be directly implemented in complex matrixes to provide sound and relevant structural information about targeted compounds prior to their purification. Although no substitute for NMR, LC-$HRMS^n$ could become a complementary tool for elucidating the chemical structures of new natural compounds.

4. Conclusion

The methodology developed in this paper aimed at exploring the chemical diversity of oak wood as an alternative to organic synthesis in the search for structural analogs of previously identified sweeteners. An original LC-HRMS-guided approach was developed by screening oak wood extracts and by combining both CPC and HPLC to purify the targeted compounds. Four new compounds were isolated and their structural elucidation was achieved, thereby revealing two isomers, one glucosyl-derivative and one galloyl-derivative of QTT I/II. These results demonstrate the pertinence of this approach since two new sweeteners were discovered in an analytical manner, without resorting to the conventional use of chemical synthesis. Moreover, HRMS developments showed that this technique can provide crucial information about the nature and sequence of functional groups in a molecule. This tool can also be used on a complex matrix, a feature that holds promise for discovering natural taste-active and bio-active compounds.

Acknowledgment

NMR experiments were performed at the Plateforme Métabolome-Fluxome, Centre de Génomique Fonctionnelle de Bordeaux, Bordeaux, France. The authors would like to acknowledge the Conseil Interprofessionnel des Vins de Bordeaux, France AgriMer Seguin-Moreau cooperage and Rémy-Martin for funding this project. They thank Lauriane Sindt for graphical assistance and Dr. Ray Cooke for proofreading the manuscript.

References

[1] R. Ferrarini, C. Carbognin, E.M. Casarotti, E. Nicolis, A. Nencini, A.M. Meneghini, The emotional response to wine consumption, Food Qual. Prefer. 21 (2010) 720–725.

[2] W.V. Parr, M. Mouret, S. Blackmore, T. Pelquest-Hunt, I. Urdapilleta, Representation of complexity in wine: influence of expertise, Food Qual. Prefer. 22 (2011) 647–660.

[3] P. Ribéreau-Gayon, Y. Glories, A. Maujean, D. Dubourdieu, The chemistry of wine stabilization and treatments, Handbook of Enology, 2, Jon Wiley & Son, Chichester, England, 2006.

[4] S.T. Lund, J. Bohlmann, The molecular basis for wine grape quality – a volatile subject, Science 311 (2006) 804–805.

[5] T.E. Acree, R.M. Butts, R.R. Nelson, C.Y. Lee, Sniffer to determine the odor of gas chromatographic effluents, Anal. Chem. 48 (1976) 1821–1822.

[6] C.M. Delahunty, G. Eyres, J.P. Dufour, Gas chromatography-olfactometry, J. Sep. Sci. 29 (2006) 2107–2125.

[7] C. Muñoz-González, J.J. Rodríguez-Bencomo, M.V. Moreno-Arribas, M.Á. Pozo-Bayón, Beyond the characterization of wine aroma compounds: looking for analytical approaches in trying to understand aroma perception during wine consumption, Anal. Bioanal. Chem. 401 (2011) 1501–1516.

[8] P. Polášková, J. Herszage, S.E. Ebeler, Wine flavor: chemistry in a glass, Chem. Soc. Rev. 37 (2008) 2478–2489.

[9] A. Glabasnia, T. Hofmann, Identification and sensory evaluation of dehydroand deoxy-ellagitannins formed upon toasting of oak wood (*Quercus alba* L.), J. Agric. Food Chem. 55 (2007) 4109–4118.

[10] J.C. Hufnagel, T. Hofmann, Orosensory-directed identification of astringent mouthfeel and bitter-tasting compounds in red wine, J. Agric. Food Chem. 56 (2008) 1376–1386.

[11] M.P. Sáenz-Navajas, P. Fernández-Zurbano, V. Ferreira, Contribution of nonvolatile composition to wine flavor, Food Rev. Int. 28 (2012) 389–411.

[12] C. Simon, K. Barathieu, M. Laguerre, J.M. Schmitter, E. Fouquet, I. Pianet, E.J. Dufourc, Three-dimensional structure and dynamics of wine tannin–saliva protein complexes. A multitechnique approach, Biochemistry 42 (2003) 10385–10395.

[13] J.L. Wolfender, G. Marti, E.F. Queiroz, Advances in techniques for profiling crude extracts and for the rapid identification of natural products: dereplication, quality control and metabolomics, Curr. Org. Chem. 14 (2010) 1808–1832.

[14] R.D. Gougeon, M. Lucio, M. Frommberger, D. Peyron, D. Chassagne, H. Alexandre, F. Feuillat, A. Voilley, P. Cayot, I. Gebefügi, N. Hertkorn, P. Schmitt-Kopplin, The chemodiversity of wines can reveal a metabologeography expression of cooperage oak wood, Proc. Natl. Acad. Sci. U. S. A. 106 (2009) 9174–9179.

[15] K.M. Kalili, J. Vestner, M.A. Stander, A. De Villiers, Toward unraveling grape tannin composition: application of online hydrophilic interaction chromatography × reversed-phase liquid chromatography-time-of-flight mass spectrometry for grape seed analysis, Anal. Chem. 85 (2013) 9107–9115.

[16] C. Roullier-Gall, M. Lucio, L. Noret, P. Schmitt-Kopplin, R.D. Gougeon, How subtle is the terroir effect? Chemistry-related signatures of two climats de Bourgogne, PLoS One 9 (2014).

[17] J. Rubert, O. Lacina, C. Fauhl-Hassek, J. Hajslova, Metabolic fingerprinting based on high-resolution tandem mass spectrometry: a reliable tool for wine authentication? Anal. Bioanal. Chem. (2014).

[18] A. Marchal, P. Waffo-Téguo, E. Génin, J.M. Mérillon, D. Dubourdieu, Identification of new natural sweet compounds in wine using centrifugal partition chromatography-gustatometry and Fourier transform mass spectrometry, Anal. Chem. 83 (2011) 9629–9637.

[19] A.D. Kinghorn, D.D. Soejarto, Discovery of terpenoid and phenolic sweeteners from plants, Pure Appl. Chem. 74 (2002) 116 9 –117 9.

[20] W. Spillane, J.B. Malaubier, Sulfamic acid and its N- and O-substituted derivatives, Chem. Rev. 114 (2014) 2507–2586.

[21] A. Bassoli, G. Borgonovo, G. Morini, Lost and found in sweeteners: forgotten molecules and unsolved problems in the chemistry of sweet compounds, Flavour Frag. J. 26 (2011) 269–273.

[22] A. De Capua, M. Goodman, Y. Amino, M. Saviano, E. Benedetti, Conformation analysis of aspartame-based sweeteners by NMR spectroscopy, molecular dynamics simulations, and X-ray diffraction studies, ChemBioChem 7 (2006) 377–387.

[23] T. Machinami, T. Fujimoto, A. Takatsuka, T. Mitsumori, T. Toriumi, T. Suami, L. Hough, Design and synthesis of new sweeteners, Pure Appl. Chem. 74 (2002) 1219–1225.

[24] M. Alías, M. Lasa, P. López, J.I. García, C. Cativiela, Aspartame analogues containing 1-amino-2-phenylcyclohexanecarboxylic acids (c6Phe). Part 2, Tetrahedron 61 (2005) 2913–2919.

571 [25] G.E. DuBois, L.A. Bunes, P.S. Dietrich, R.A. Stephenson, Diterpenoid sweeteners.
572 Synthesis and sensory evaluation of biologically stable analogues of stevioside, J. Agric. Food
573 Chem. 32 (1984) 1321–1325.
574 [26] J. Hong, Role of natural product diversity in chemical biology, Curr. Opin. Chem. Biol. 15
575 (2011) 350–354.
576 [27] J.V. Olsen, B. Macek, O. Lange, A. Makarov, S. Horning, M. Mann, Higher-energy C-trap
577 dissociation for peptide modification analysis, Nat. Methods 4 (2007) 709–712.
578 [28] Y. Xu, J.F. Heilier, G. Madalinski, E. Genin, E. Ezan, J.C. Tabet, C. Junot, Evaluation of
579 accurate mass and relative isotopic abundance measurements in the LTQ-Orbitrap mass
580 spectrometer for further metabolomics database building, Anal. Chem. 82 (2010) 5490–5501.
581 [29] A.P. Foucault, L. Chevolot, Counter-current chromatography: instrumentation, solent
582 selection and some recent applications to natural product purification, J. Chromatogr. A 808
583 (1998) 3–22.
584 [30] K.E. Kövér, V.J. Hruby, D. Uhrín, Sensitivity- and gradient-enhanced heteronuclear
585 coupled/decoupled HSQC-TOCSY experiments for measuring longrange heteronuclear
586 coupling constants, J. Magn. Reson. 129 (1997) 125–129.
587 [31] C. DeAmicis, N.A. Edwards, M.B. Giles, G.H. Harris, P. Hewitson, L. Janaway, S.
588 Ignatova, Comparison of preparative reversed phase liquid chromatography and countercurrent
589 chromatography for the kilogram scale purification of crude spinetoram insecticide, J.
590 Chromatogr. A 1218 (2011) 6122–6127.
591 [32] S.Y. Shi, M.J. Peng, Y.P. Zhang, S. Peng, Combination of preparative HPLC and HSCCC
592 methods to separate phosphodiesterase inhibitors from *Eucommia ulmoides* bark guided by
593 ultrafiltration-based ligand screening, Anal. Bioanal. Chem. 405 (2013) 4213–4223.
594 [33] A. Berthod, Countercurrent Chromatography, Vol. 38, Elsevier, 2002.
595 [34] O. Frank, H. Ottinger, T. Hofmann, Characterization of an intense bitter-tasting 1H,4H-
596 quinolizinium-7-olate by application of the taste dilution analysis, a novel bioassay for the
597 screening and identification of taste-active compounds in foods, J. Agric. Food Chem. 49
598 (2001) 231–238.
599 [35] H. Hillmann, J. Mattes, A. Brockhoff, A. Dunkel, W. Meyerhof, T. Hofmann, Sensomics
600 analysis of taste compounds in balsamic vinegar and discovery of 5-acetoxymethyl-2-
601 furaldehyde as a novel sweet taste modulator, J. Agric. Food Chem. 60 (2012) 9974–9990.
602 [36] S. Scharbert, N. Holzmann, T. Hofmann, Identification of the astringent taste compounds
603 in black tea infusions by combining instrumental analysis and human bioresponse, J. Agric.
604 Food Chem. 52 (2004) 3498–3508.

[37] R. Lopez, L. Mateo-Vivaracho, J. Cacho, V. Ferreira, Optimization and validation of a taste dilution analysis to characterize wine taste, J. Food Sci. 72 (2007).

[38] P. Arapitsas, G. Speri, A. Angeli, D. Perenzoni, F. Mattivi, The influence of storage on the chemical age of red wines, Metabolomics 810 (2014) 816–832.

[39] R.D. Gougeon, M. Lucio, A. De Boel, M. Frommberger, N. Hertkorn, D. Peyron, D. Chassagne, F. Feuillat, P. Cayot, A. Voilley, I. Gebefügi, P. Schmitt-Kopplin, Expressing forest origins in the chemical composition of cooperage oak woods and corresponding wines by using FTICR-MS, Chem. Eur. J. 15 (2009) 600–611.

[40] X. Li, G. Servant, Functional Characterization of the Human Sweet Taste Receptor: High-Throughput Screening Assay Development and Structural Function relation, in: D.K. Weerasinghe, G.E. DuBois (Eds.), Sweetness and sweeteners, ACS Symposium Series No. 979, Oxford University Press, New York, 2008, pp. 368–385.

[41] X. Li, L. Staszewski, H. Xu, K. Durick, M. Zoller, E. Adler, Human receptors for sweet and umami taste, Proc. Natl. Acad. Sci. U. S. A. 99 (2002) 4692–4696.

[42] A.D. Kinghorn, L. Pan, J.N. Fletcher, H. Chai, The relevance of higher plants in lead compound discovery programs, J. Nat. Prod. 74 (2011) 1539–1555.

[43] M. Zehl, E. Pittenauer, L. Jirovetz, P. Bandhari, B. Singh, V.K. Kaul, A. Rizzi, G. Allmaier, Multistage and tandem mass spectrometry of glycosylated triterpenoid saponins isolated from *Bacopa monnieri*: comparison of the information content provided by different techniques, Anal. Chem. 79 (2007) 8214–8221.

[44] F. Cuyckens, M. Claeys, Mass spectrometry in the structural analysis of flavonoids, J. Mass Spectrom. 39 (2004) 1–15.

Figures

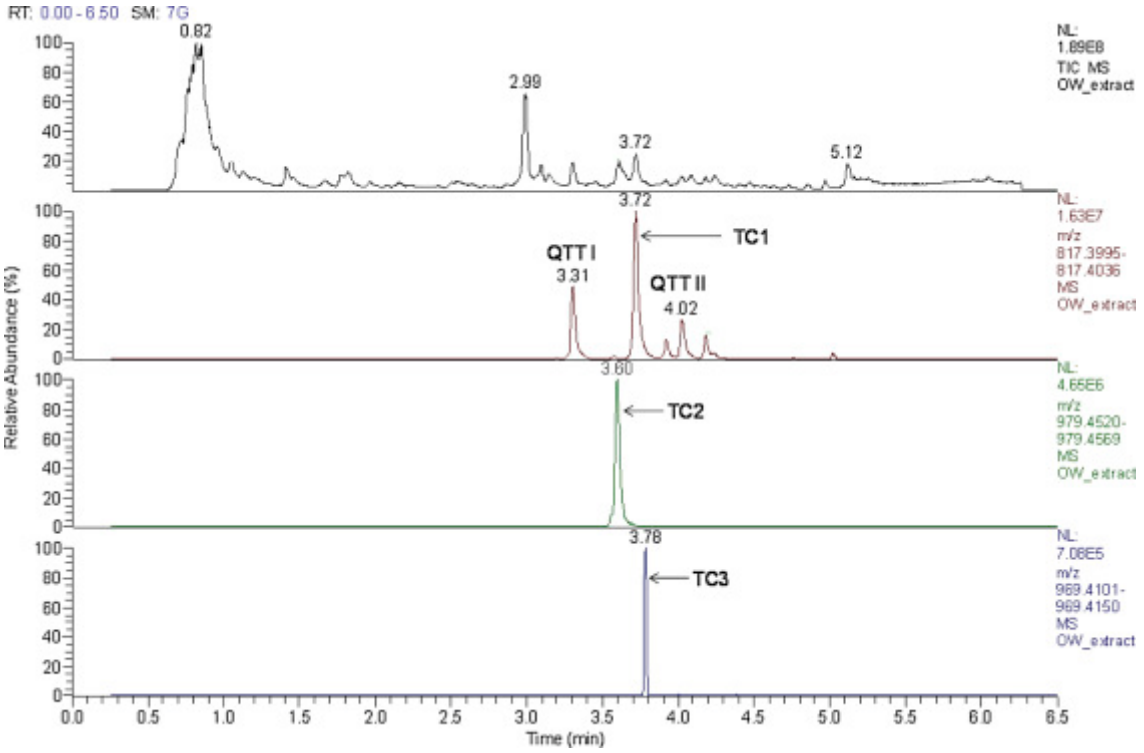

Figure 1. LC-HRMS screening of an oak wood extract. From top to bottom: TIC and XICs chromatograms for isomers, MonoHex and MonoGall derivatives of **QTTI/II**. XICs were recorded in a 5 ppm window.

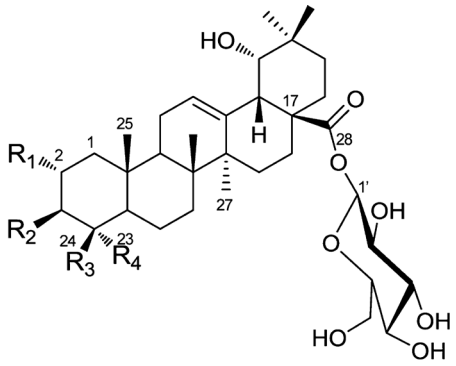

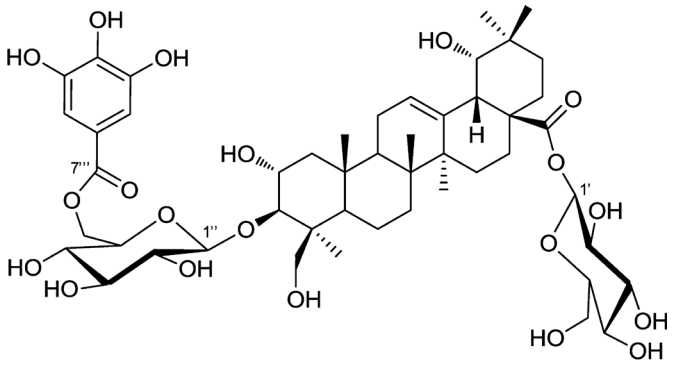

	R_1	R_2	R_3	R_4
QTT I	OH	OH	CH_3	CH_2OGall
QTT II	OH	OGall	CH_2OH	CH_3
QTT III	OH	OGall	CH_3	CH_2OH
QTT V	OH	OGall $_{7''}$	CH_3	$CH_2OGall_{7'''}$
QTT VI	OGall	OH	CH_3	CH_2OH

QTT IV

Gall = galloyl

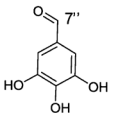

Figure 2. Chemical structures of QTT isomers and derivatives.

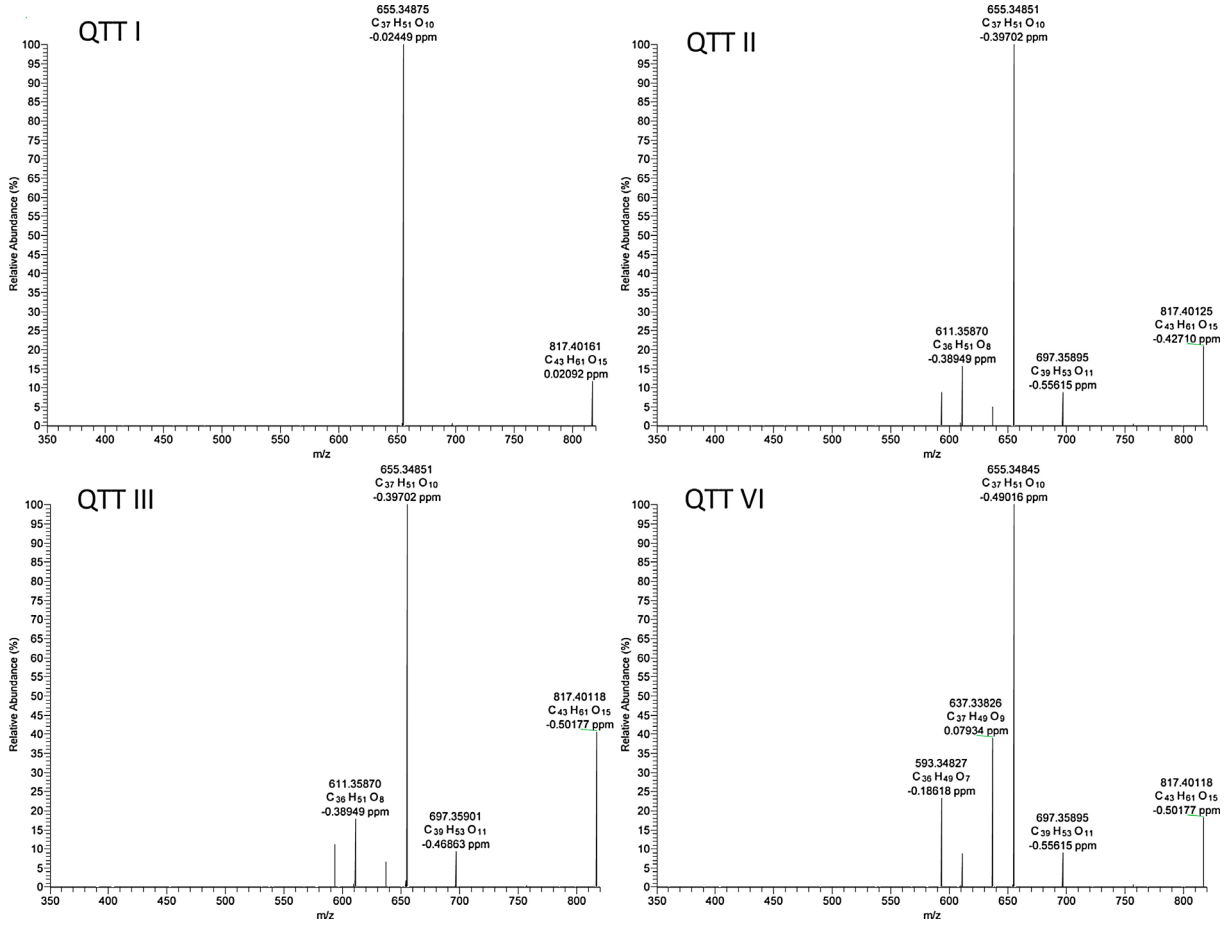

Figure 3. LIT CID MS^2 spectra at 25% resonant collision energy of the $[M–H]^-$ ion of **QTT I**, **II**, **III** and **VI**.

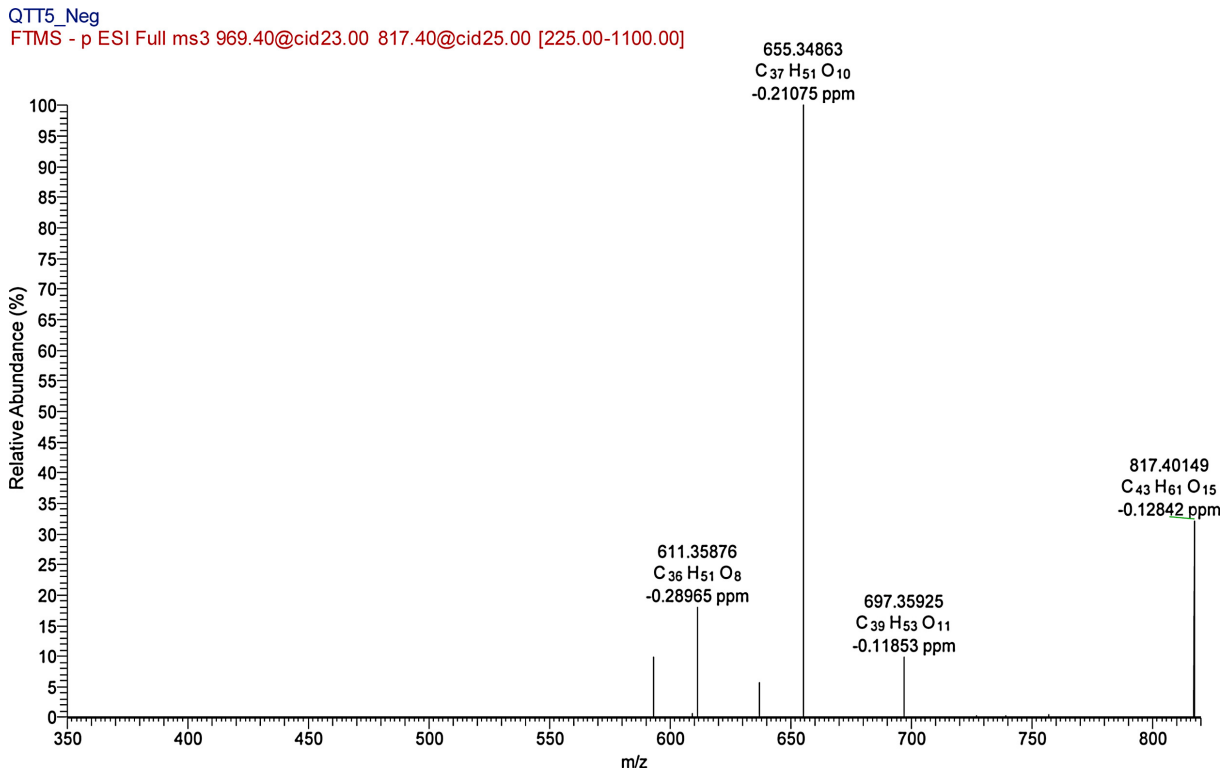

Figure 4. LIT CID MS^3 spectrum of a fragment ion from **QTT V** at *m/z* 817 that corresponded to the genin functionalized with one hexosyl and one galloyl group.

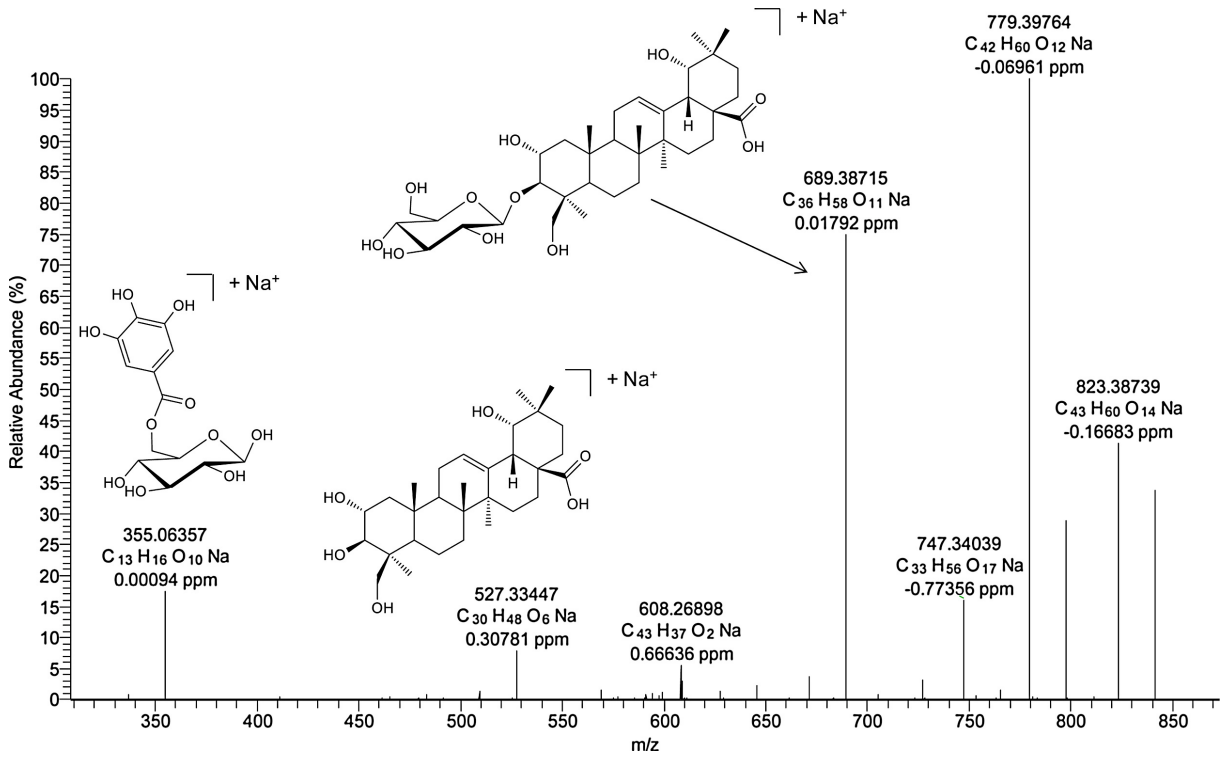

Figure 5. LIT CID MS^3 spectrum of the *m*/*z* 841 product ion of **QTT IV** ($[M–Glu + Na]^+$) at 29 eV. The concomitant presence of fragments at *m*/*z* 355.0636 and 689.3871 clearly established the sequence Gall–Glu–Genin

Tables

Table 1. Ionization and spectrometric conditions for HRMS analyses.

Mass spectrometer	**Exactive**	**LTQ-Orbitrap Elite**		
Use	**LC-MS**	**Direct infusion**		**LC-MS^n**
Ionization mode	**Negative**	**Negative**	**Positive**	**Negative**
Sheath gas flow[a]	75	20	3	80
Auxiliary gas flow[a]	15	5	5	10
HESI probe temperature	320 °C	50 °C	50 °C	50 °C
Capillary temperature	350 °C	350 °C	350 °C	350 °C
Electrospray voltage	−3.5 kV	−3 kV	3 kV	−3 kV
Capillary voltage	−95 V	–	–	–
Tube lens voltage offset	−190 V	–	–	–
Skimmer voltage	−46 V	–	–	–
S-Lens RF level	–	60%	60%	60%
Mass range (in Th)	400–1900	100–1500	100–1500	100–1500
Resolution[b]	25,000	120,000	120,000	30,000
AGC value	10^6	2.10^5	2.10^5	2.10^5

[a]Sheath gas and auxiliary gas flows (both nitrogen) are expressed in arbitrary units.

[b]Resolution $m/\Delta m$, fwhm at m/z 200 Th for exactive and at at m/z 400 Th for LTQ-Orbitrap.

Table 2. Empirical formulae and $[M–H]^-$ theoretical masses of **QTT I/II** isomers and derivatives.

Relation to QTT I and II[a]	**Empirical formula**	**$[M–H]^-$ theoretical mass**
Isomers	$C_{43}H_{62}O_{15}$	817.4016
MonoHex derivatives	$C_{49}H_{72}O_{20}$	979.4544
DiHex derivatives	$C_{55}H_{82}O_{25}$	1141.5072
MonoGall derivatives	$C_{50}H_{66}O_{19}$	969.4126
DiGall derivatives	$C_{57}H_{70}O_{23}$	1121.4235
MonoHex-MonoGall derivatives	$C_{56}H_{76}O_{24}$	1131.4654

[a]Hex for hexosyl, Gall for galloyl.

Table 3. ^{1}H and ^{13}C NMR data of **QTT III–VI** in CD_3OD.

Genin	**QTT III**		**QTT IV**		**QTT V**		**QTT VI**	
	δ_C	$\delta_{H(J = Hz)}$	δ_C	$\delta_{H(J = Hz)}$	δ_C	$\delta_{H(J = Hz)}$	δ_C	$\delta_{H(J = Hz)}$
1	46.7	1.06 m	45.4	0.87 m	47	1.14 m	43.2	1.03 m
		2.01 dd (12.6; 4.7 Hz)		1.96 dd (13.2; 3.8 Hz)		2.06 dd (12.5; 4.6 Hz)		2.06 dd (4.7; 12.2 Hz)
2	66.4	3.99 td (9.9; 4.7 Hz)	66.7	3.82 m	66.4	4.02 td (10.1; 4.6 Hz)	72.9	5.21 dd (4.7; 10.7 Hz)
3	78.7	5.05 d (9.9 Hz)	94.4	3.21 d (9.9 Hz)	78.5	5.24 d (10.1 Hz)	73.5	3.77 d (10.7 Hz)
4	43.3		44.9		42.7		43.5	
5	46.5	1.53 brd (11.4 Hz)	55.7	1.05 m	47.9	1.46 m	46.7	1.44 m
6	17.8	1.46 td (13.0; 2.7 Hz)	18.4	1.46 td (13.2; 2.3 Hz)	17.9	1.48 m	17.6	1.46 m
		1.53 m		1.63 m		1.52 m		1.53 m
7	31.8	1.33 m	32.8	1.34 m	32	1.28 m	31.7	1.32 m
		1.69 m		1.54 m		1.43 m		1.66 m
8	39.4		39.6		39.4		38.8	
9	47.6	1.92 t (8.6 Hz)	47.5	1.77 m	48	1.88 t (9.3 Hz)	47.8	1.87 m
10	37.6		37.1		37.7		38.6	
11	23.2	2.04 m	23.8	1.76 m	23.5	2.04 m	23.3	1.96 m
				2.01 m				2.01 m
12	123.4	5.36 t (3.3 Hz)	123	5.34 t (3.3 Hz)	123.1	5.34 t (3.41)	123.3	5.33 t (3.5 Hz)
13	142.6		142.8		143.3		143.1	
14	41.4		41.2		41.2		42.7	
15	27.4	1.74 m	27.8	1.01 m	27.9	0.96 m	27.5	1.03 m
				1.68 m		1.62 m		1.32 m
16	27.1	1.74 m	27.6	1.73 m	27	1.71 m	26.6	1.73 m
		2.35 td (13.4; 4.1 Hz)		2.33 td (13.5; 3.9 Hz)		2.3 td (13.2; 3.6 Hz)		2.34 td (4.2; 13.2 Hz)
17	45.6		45.7		45.7		45.6	
18	43.7	3.07 d (4.1 Hz)	43.9	3.07 d (3.9 Hz)	43.6	3.06 bd	44	3.07 d (3.4 Hz)
19	81.1	3.29 d (4.1 Hz)	81	3.29 d (3.9 Hz)	81	3.27 d (3.8 Hz)	81	3.28 d (3.4 Hz)

20	34.3		34.4		34.3		34.7
21	28	1.03 m	28	1.02 m	28.1	1.03 m	27.5	1.03 m
		1.70 m		1.79 m		1.77 m		1.69 m
22	31.7	1.66 m	32.1	1.70 m	31.8	1.67 m	31.7	1.66 m
		1.76 m		1.82 m		1.77 m		1.78 m
23	63.7	3.01 d (11.9 Hz)	21.9	1.25 s	64.9	3.53 d (11.9 Hz)	64	3 .33 m
		3.32 d (11.9 Hz)				4.32 d (11.9 Hz)		3.55 d (11.4 Hz)
24	13.7	0.86 s	63.1	3.41 d (11.4 Hz)	13.1	1.06 s	12.6	0.79 s
				3.92 d (11.4 Hz)				
25	16.3	1.11 s	15	0.92 s	16	1.14 s	15.7	1.15 s
26	16.4	0.79 s	16.2	0.75 s	16.4	0.78 s	16.3	0.79 s
27	23.3	1.34 s	23.4	1.29 s	23.5	1.20 s	23.4	1.32 s
28	177.1		177		176.9		177.1	
29	23.8	0.97 s	27.2	0.95 s	23.8	0.96 s	26.9	0.95 s
30	27.3	0.96 s	24.2	0.96 s	27.1	0.95 s	23.6	0.96 s
28-β-D-glucose								
1′	94.4	5.39 d (8.2 Hz)	94.2	5.38 d (8.1 Hz)	94.5	5.38 d (8.1 Hz)	94.4	5.39 d (8.4 Hz)
2′	72.6	3.34 m	72.6	3.32 m	72.7	3.32 m	72.2	3.33 m
3′	77.9	3.34 m	77.3	3.35 m	77.2	3.36 m	77.1	3.36 m
4′	69.6	3.36 m	69.6	3.35 m	69.5	3.36 m	69.7	3.38 m
5′	77.3	3.36 m	77	3.41 m	76.8	3.41 m	76.9	3.40 m
6′	60.9	3.69 dd (11.8; 4.3 Hz)	60.9	3.69 dd (11.9; 4.3 Hz)	60.8	3.69 dd (11.7; 4.3 Hz)	60.6	3.69 dd (4.4; 12.2 Hz)
		3.82 brd (11.8 Hz)		3.82 brd (11.9 Hz)		3.83 brd (11.7 Hz)		3.83 brd (12.2 Hz)
			3-β-D-glucose					
1″			104.2	4.51 d (8.2 Hz)				
2″			74.3	3.30 m				
3″			76.4	3.46 m				
4″			70.2	3.47 m				

5″			74.4	3.68 m				
6a″			62.7	4.38 dd (12.1; 5.2 Hz)				
6b″				4.63 dd (12.1; 2.1 Hz)				
	3-galloyl		6″-galloyl		3-galloyl		2-galloyl	
1‴	120.4		119.3		120.5		120.7	
2‴/6‴	108.2	7.12 s	108.5	7.11 s	108.8	7.12 s	108.7	7.10 s
3‴/5‴	145.1		144.8		145		144.6	
4‴	138.1		138.7		138.2		138.2	
7‴	167.5		166.4		166.9		167.1	
1⁗					120.1			
2⁗/6⁗					108.8	7.16 s		
3⁗/5⁗					145.1			
4⁗					138.4			
7⁗					166.4			